International Journal of Engineering

Journal Homepage: www.ije.ir

Ultimate Unbonded Tendon Stress in CFRP Strengthened Post-Tensioned Indeterminate I-Beams Cast with HSCs

A. A. Maghsudi*, Y. Askari D.

Department of Civil Engineering, Shahid Bahonar University, Kerman, Iran

PAPER INFO

Paper history:
Received 31 August 2014
Received in revised form 14 January 2015
Accepted 30 January 2015

Keywords:
Strengthened
CFRP Sheet
Unbonded Tendons
Stress Increases
High Strength Normal
Self-Compacting Concrete
Continuous Beams

A B S T R A C T

Based on the bending experiment for two-span continuous post-tension beams with unbounded tendons and externally applied CFRP sheets, the analysis of the stress increment of unbonded tendons is monitored in the loading process. Since self-compacting concrete (SCC) is a suitable innovation,, understanding the implementation of this type of concrete on the ultimate unbonded tendon stress is critical. For these aims, results of four continuous un-bonded post-tensioned I-beams in two groups were cast and monitored by electrical strain gauges andare presented here. In the first group, the beams (UPN1-12, SUPN1-12) consisted of high strength normal concrete (HSNC), while in the second group (UPS1-12, SUPS1-12) high strength self-compacting concrete (HSSCC) were tested. The beams are made which are compared with the theory proposed by different codes, and a preliminary modification is given for each code equation. The results of standard error of estimate $S_{y/x}$, indicates that for two types of HSCs (strengthened and non-strengthened beams), the ACI 318-2011 provides better estimates than AASHTO-2010 model, whereas this model provides better estimates as compared toBS 8110-97.Comparison of increase in experimental ultimate tendon stress of beams indicates that the increase in tendon stress at ultimate state in strengthened beams is lower than that in non-strengthened beams cast with HSCs.

***doi**: 10.5829/idosi.ije.2015.28.03c.03*

1. INTRODUCTION

Post-tensioned high strength concrete beams with unbonded tendons and externally applied CFRP sheets is a kind of new technique for strengthening and has the merits of both post-tensioned unbonded prestressed HSCs and strengthening with externally CFRP sheets. To analysis and perform flexural design of such concrete members with unbounded tendons, the ultimate stress in the prestressed steel must be known. Due tolack of continuity between unbounded tendons and surrounding concrete, the theory of strain compatibility cannot be applied to the strain of unbonded tendons in such concrete beams subjected to loading. Therefore, estimation of stress increase in the tendons due to external loading is difficult. In the case of post-tensioned members hundreds of elements, both slabs and beams cast with normal (vibrated) concrete were tested by Harajli and Kanj [1], Lim et al. [2], Ozkul et al. [3], Yang and Mun [4] and other researchers. Through these investigations, there were separated parameters thathave influence on the stress increment in unbonded tendons. These are: span-to-depth ratio, concrete compressive strength (normal and high strength vibrated concrete), yield strength, tendon profile, tensile strength and amount of non-prestressed and prestressed reinforcement, type of loading (single point load, third-point loading and uniformly distributed load), loading pattern in continuous members (uniform loading, alternate spans, adjacent spans, external span or internal span) and stress in the tendon after time-dependent losses. These parameters have caused formulating of tendon stress more complicated. Since the early 1950s, researchers have suggested many experimental and analytical equations to predict the stress in unbonded tendon at an ultimate state, which

*Corresponding Author's Email: maghsoudi.a.a@uk.ac.ir (A. A. Maghsudi)

Please cite this article as: A. A. Maghsudi and Y. Askari D., Ultimate Unbonded Tendon Stress in CFRP Strengthened Post-Tensioned Indeterminate I-Beams Cast with HSCs, International Journal of Engineering (IJE), TRANSACTIONS C: Aspects Vol. 28, No. 3, (March 2015) 350-359

have been evaluated and reviewed by Harajli and Kanj [1]; He and Liu [5]; Zhou and Zheng [6]. However, these equations donot take into account all important parameters and work with vibrated nearly low strength concrete. Compared to conventional (vibrated) concrete, self-compacting concrete(SCC) is a new type of concrete that is able to flow and compact under its own weight, completely fill the formwork even in the presence of congested reinforcement, whilst maintaining homogeneity without need forinternal or external compaction. This has generated tremendous interest since initial development in Japan by Okamura in the 1986 in order to reach durable concrete structures.In contrast with Japan, research in Europe, America and Iran has started only recently [7].The good workability, high rate of production and durability assurance of SCC create wide acceptance by the prestressed and precast concrete industry where congestion of reinforcement is the norm (PCI Self-Consolidating Concrete FAST Team [8]). Many prestressed and precast concrete producers currently use SCC for 100%or a considerable part of their production (Walraven [9]). SCC shortens the construction period and assures full compaction in the confined zones in the prestressed concrete structures especially the end-blocks of prestressed concrete structures, where concrete compaction by vibration, due to large amount of steel reinforcement is difficult. With recent advancements in concrete technology, and the availability of various types of mineral and chemical admixtures and very powerful superplasticizers, both vibrated and non-vibrated concrete with a compressive strength of up to 100 MPa can now be produced commercially with an acceptable level of variability using ordinary aggregates.Material properties may have important consequences in terms of structural behavior and design of HSC members. Hashemi et al. [10] studied some of these structural behaviors, including flexural ductility. Since HSCs is well accepted for prestressed concrete construction, it is necessary that more data and information on ultimate stress increase in unbonded tendons in HSCs (especially HSSCC, which is nearly a new invitation) post-tensioned members be available. Fiber reinforced polymer (FRP) composite materials have been developed into economically and structurally viable construction materials for buildings and bridges over the past25 years [11]. Externally bonding fiber FRP sheets with an epoxy resin is an effective technique for strengthening and repairing the reinforced concrete (RC) beams under flexural loads (Akbarzadeh et al. [12]. However, no report is available on the effect of externally bonding FRP on the ultimate unbonded tendon stress in post-tensioned indeterminate beams cast with HSNC and HSSCC. The purpose of this research is to deliver information about behavior of members cast with HSNC and HSSCC, prestressed with unbonded tendons and strengthened by externally bonding FRP sheets. The conclusion of this paper can provide the reference data for the design of such prestressed concrete continuous members.

2. EXPERIMENTAL PROGRAM

Four unbounded post-tensioned I-beams were cast and tested in two group. In the first group, the beams (UPN1-12, SUPN1-12) consisted of HSNC where as in the second group the beams (UPS1-12, SUPS1-12) were made of HSSCC. In each group, one beam served as control (UPN1-12, UPS1-12) while the other two (SUPN1-12, SUPS1-12) strengthened with CFRP sheets in both sagging and hogging regions.Here, the letter U is stands for unbonded, P is for post-tensioned, N and S is for normal and self-compacting concrete and the letter S appeared before U, is stands for beams strengthened by FRP. The beams were designed based on ACI-318-11 [13] for conventional (vibrating) concrete.

2. 1. Mix Design and Fresh Concrete Properties

The key point to achieve self-compacting property of concrete is providing high flowability and deformability, while maintaining resistance to segregation and sedimentation. This can be achieved by proper balance between constituent materials. Okamura et al. [14] proposed limiting of volume of coarse aggregates, along with use of high amount of powders, controlling the water/powder ratio by volume and use of proper super-plasticizers to achieve, SCC. Domone [15] showed the wide use of these mixing rules in application with a wide statistical analysis on 68 commercial projects through the world. In his study, the experimental program involves two different types of concrete, HSSCC and HSNC, with a similar target compressive strength of 90 MPa; two different mixes with nearly one class of compressive strengths have been designed with a specific surface (Blaine) of Portland cement as 3100 cm^2/gr (the full detailsof mix design is presented in [16]).

2. 2. Plastic and Hardened Concrete Phase Results And Discussion

For beams consisting of normal concrete, an average slump of 6.5cm was obtained. Whereas, for beams consisting HSSCC, the necessary tests were carried out on the fresh concrete to check the self-compacting properties of mixes. This included J ring, V funnel, L box tests, slump flow diameter and flow velocity T_{50}. The tests results on plastic phase of SCC were evaluated with the precast/prestressed concrete institute (PCI) guidelines for SCC [17]. Also, it was considered as a reference, and it was concluded that the designed mix can be considered as SCC in plastic phase. Therefore, it is used to cast industrial the second group of post-tensioned beams (UPS1-12, SUPS1-12). In hardened phase of concrete, compressive strength was measured. Cylinder specimens were made for compressive tests. Tests were carried out at two ages (i.e., transfer of prestressed force as well as 28 day) and an average value of three specimens was considered as 90 and 94 MPa for HSSCC and HSNC respectively (see in Table 1).

2. 3. Unbonded Post-tensioned Beams Fabrication

2. 3. 1. Tendons Preparation The 13.9 mm diameter tendons (consisting of 7 wires) were cut to the required length of 10 meter. Three locations (designated as A, B, C) along the prestressing tendons were smoothenedand cleaned and the electrical strain gauges were installed at this locations As shown in Figure 1.. One electrical strain gauge type FLK-2-11-5LT is attached on each location of A, B and C. The profile of the tendon (laying pattern) consisting of variable tendon eccentricity of beams is presented by Equation (1):

$$e(x) = \begin{cases} -0.027x^3 + 0.0822x^2 + 0.0265x + 0.002 & 0 \le x \le 2.175 \\ 0.0661x^3 - 0.6468x^2 + 1.8759x - 1.53 & 2.175 \le x \le 4.35 \end{cases} \quad (1)$$

2. 3. 2. Beam Specimens The design variables and summary of the test beams is provided in Table 3. The typical dimensions and relevant reinforcement details of beams are shown in Figure 1. The areas of the ordinary reinforcement and the prestressing steel were selected to produce reinforcing indexes within the practical range of design.

2. 4. Prestressing Method, Monitoring and Measurements of Prestressed Beams

The prestressing method was post-tensioning unbonded system. Post-tensioning was carried out 7 days after concrete casting. The electrical strain gauges mounted on the tendons were connected to the data acquisition system. The data acquisition system monitored and recorded the tendon strains during jacking and loading operation to the computer system for further analysis.

The tendons were tensioned to required jacking force using a 22-ton capacity hydraulic jack. The prestressing operation is shown in Figure 1. However, the losses of prestresed forces evaluated and reported elsewhere by Askari and Maghsudi [31].

TABLE1. Summary of test parameters

Beams	$f'_{c,i}$ (MPa) transfer age	$f'_{c,28}$ (MPa)	Steel bars: A_s Midspan and internal support (mm^2)	Steel bars: A'_s Midspan and internal support (mm^2)	Prestressed steel strand: A_p (mm^2)	Prestressed steel strand: d_p Midspan (mm)	Prestressed steel strand: d_p Internal support (mm)
UPN1-12	80	95	2ø12 (226)	2ø12 (226)	1 (0.6 in) 140	370	370
SUPN1-12	79	93	2ø12 (226)	2ø12 (226)	1 (0.6 in) 140	370	370
UPS1-12	76	90	2ø12 (226)	2ø12 (226)	1 (0.6 in) 140	370	370
SUPS1-12	75	89	2ø12 (226)	2ø12 (226)	1 (0.6 in) 140	370	370

TABLE 2. Mechanical properties of the CFRP sheet.

Material	Density (gr/cm^3)	Thickness (mm)	Ultimate tensile stress, f_{fu} (MPa)	Young's modulus, E_f (MPa)	Ultimate strain, e_{fu}(%)
CFRP	1.76	0.131	4300	238000	1.8

TABLE 3. Mechanical properties of the bonding adhesive.

Material	Density (gr/cm^3)	Compressionstrength(MPa)	Tensilestrength(MPa)	Young'smodulus(MPa)	Shearstrength(MPa)
Epoxy resinadhesive	1.11	97.4	76.1	3600	54.8
Epoxy resinprimer	1.77	>90	>25	12800	>15

TABLE 4. Details of CFRP strengthening of the test specimens

Beam no.	CFRP width (mm)	Positive moment strengthening: No. of layers	Positive moment strengthening: Strengthen length (mm)	Negative moment: No. of layers	Negative moment: Strengthen length (mm)	U wrapped end anchorage
UPN1-12	-	-	-	-	-	-
SUPN1-12	200	1	6528	1	2673	Yes
UPS1-12	-	-	-	-	-	-
SUPS1-12	200	1	6528	1	2673	Yes

TABLE 5. Summary of tests results

Beam no.	$P_y(kN)$	$\xi = p_y$ *(strengthened)/* p_y *(unstrengthened)*	**Average deflectionat yielding load** (Δ_y) **(mm)**	P_u *(kN)*	$\lambda = P_u$ *(strengthened)/* p_u *(unstrengthened)*	**Average deflectionat failure load** (Δ_u) **(mm)**	**Failure Mode**
UPN1-12	172.6	1	2.45	346.6	1	26.3	Flexural manner
SUPN1-12	290	1.68	8.8	398	1.15	27	Rupture of the CFRP sheet over the central support
UPS1-12	183	1	2.83	365.3	1	31.15	Flexural manner
SUPS1-12	234	1.28	3.63	382	1.05	27.8	IC debonding at hogging region

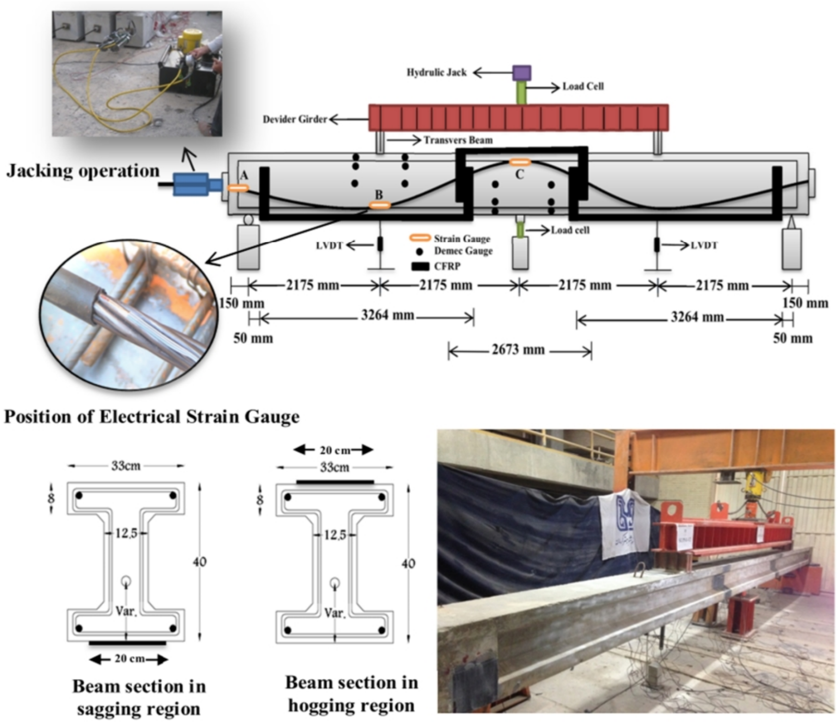

Figure 1. Typical dimensions, reinforcement details and geometry of test beams

2. 5. CFRP Properties

The Young's modulus (E_{fu}) and ultimate tensile stress (f_{fu}) of the CFRP sheet and the properties of epoxies used for bonding the CFRP sheets were obtained from the producer and are given in Table 2 and 3. Details of CFRP strengthening of the test specimens are shown in Table 4.The beams were loaded with two concentrated point loads applied simultaneously at the middle of each two spans.

Depending on the diameter of the steel bars three different types of electrical strain gauges were mounted on the main ordinary reinforced bars, stirrups and prestressing tendon at specific locations to monitor the development of conventional and prestressing steel strains throughout the loading history. The strain on concrete surface at different locations were also monitored by electrical strain gauges and mechanical demec points (steel less steel discs) 200 mm apart (Figure 1).

The control post-tensioned beam cast with HSNC, UPN1-12, failed in flexural manner. The tensile steel yielded (P_y *=172.6 kN*) prior to concrete crushing at both the central support (P_u *= 346 kN*) and mid-span section. At failure, the wide flexural cracks occurred at mid-span (w_{crmax}*=21 mm*) and central support (w_{crmax}*= 21 mm*). These cracks started at extreme concrete tensile layers and well extended to the compressive regions. The rupture of tendon was sudden and accompanied by a loud noise and shove end anchorage indicating a rapid release of energy and a total loss of load bearing capacity.

The tensile steel at central support for beam SUPN1-12 yielded at a load of *290 kN*. The load was further increased and the beam failed at a load of *398 kN* by intermediate crack (IC) debonding of CFRP sheet at hogging and sagging regions and rupture of CFRP sheet at interior support and end strap at hogging region (Figure 2). At failure, wide flexural cracks occurred at mid-span (w_{crmax}=*8 mm*) and central support (w_{crmax}= *7 mm*). By strengthening the UPN1-12 beam using CFRP sheet, the beam flexural capacity is increased and therefore, more number of flexural cracks initiatedand developed towards the neutral axis before beam failure.The tensile steel at central support of beam SUPS1-12 yielded at a load of *234 kN*. The load was applied further and the beam failed at a load of *382 kN* by intermediate crack (IC) debonding of CFRP sheet at hogging and sagging region.

At failure, the wide flexural cracks occurred at mid-span (w_{crmax}=*11 mm*) and central support (w_{crmax}= *4 mm*). The flexural capacity of the UPS1-12 beam increased and therefore, more number of flexural cracks initiatedand developed towards the neutral axis before beam failure.

Figure 2. Typical crack pattern of tested beams

Figure 3 shows the applied load versus average deflection of the right and left spans of thebeams. The beams exhibited three stage responses up to failure; representing the concrete precracking stage, concrete postcracking to tension steel preyield stage, and tension steel postyield stage to failure. In the uncracked elastic stage, the same behavior was observed for all tested beams, indicating very similar beam's stiffness prior to concrete cracking. In the cracked preyield stage, the stiffness and yield load of the CFRP strengthened beams were slightly larger than that of the control beams and no significant decreases in beam's stiffness was observed after yielding the tensile steel at sections of negative and positive moments.The moment-flexural crack width diagrams of post-tensioned beams are compared and shown in Figure 4. This figure shows that crack width is significantly reduced with strengthened post-tensioned beams. In the cracked pre yield stage and after yielding of tensile steel, the same crack width was observed for strengthened HSNC and HSSCC beams.

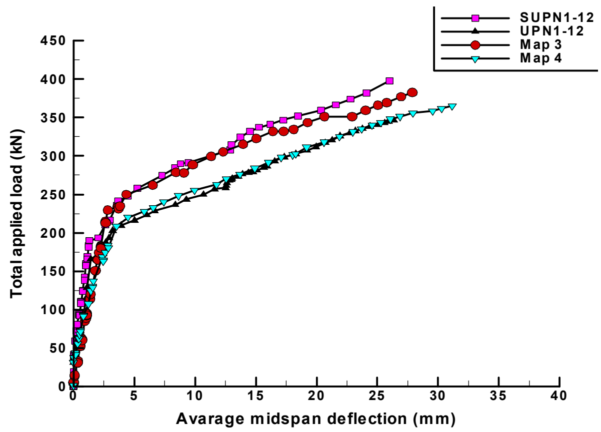

Figure 3. Applied load versus average midspan deflection

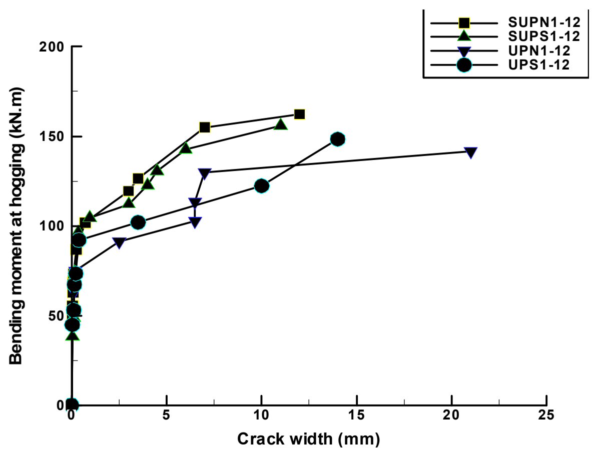

Figure 4. Flexural crack widths of strengthened and unstrengthened beams

4. RELATIONSHIP BETWEEN TOTAL LOAD P AND F_{PS} IN TESTED BEAMS.

In order to get a clear understanding of the behavior of strengthened HSSCC and HSNC beams (i.e., from jacking force up to failure load), the beams monitoring was performed.

The variation of prestressing steel stress as the load increases shown in Figure 5. For all beams the initial measured stress in tendon (at jacking operation) was $0.73f_{pu}$, after total stress losses (immediate and time depended losses after two month), the amount of measured stress in UPN1-12 reduced to $0.58f_{pu}$. During the beam load test, stress in tendon increased as load increased, and reached to a value of $0.91f_{pu}$ at ultimate load (an increase of 58%). However, the change in tendon stress during the beam load test for the SUPN1-12 beam, was *528 MPa*, increasing by 50%.

From Figure 5, the effective tendon stress monitored in the UPS1-12 beam after total stress losses registered as *1082 MPa* ($0.6f_{pu}$). During the beam load test, stress in tendon increased as load increased and experienced a value of $0.92f_{pu}$ at ultimate load (an increase of 54%).

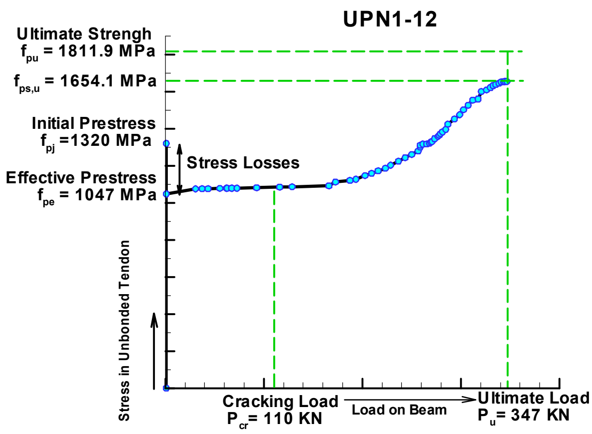

(a)

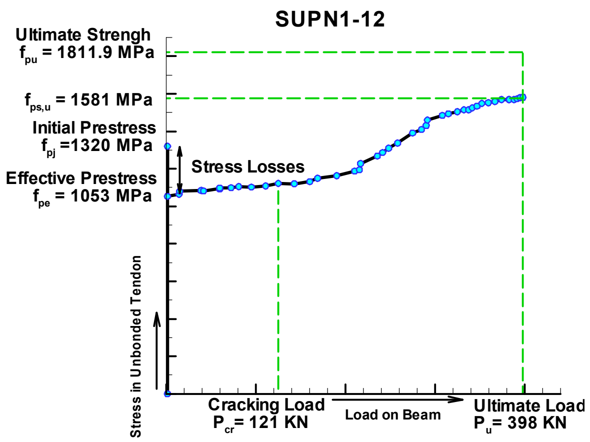

(b)

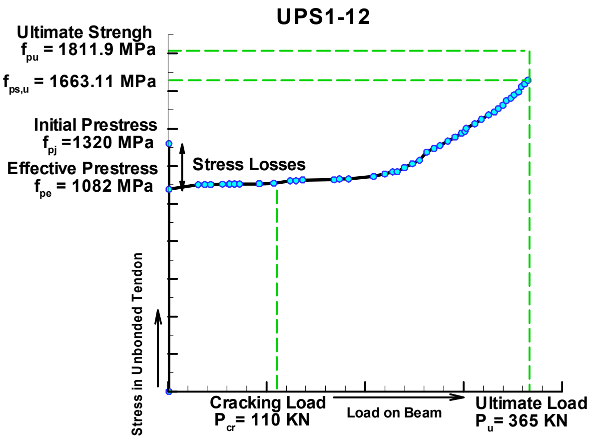

(c)

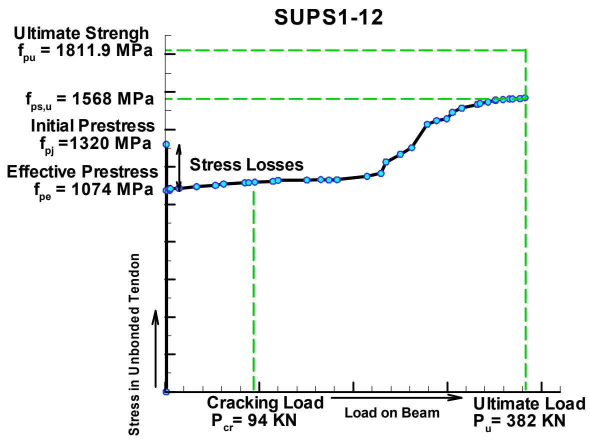

(d)

Figure 5. Variation of prestressing steel stress with applied load for tested beams

On the other hand, the SUPS1-12 beam, which was subjected to loading, registered a tendon stress increase from *1074 MPa* to *1568 MPa* (an increase of 46%). It was noted that, the increase in tendon stress was decreased by strengthening the beam with CFRP sheets for two type of concrete (HSSCC and HSNC).

5. COMPARISON OF STANDARD PREDICTION AND TEST RESULTS

The accuracy of predicted equations by relative Standards such as, ACI318-2011, AASHTO [18] and BS8110 [19] are verified with the results of beams cast with HSCs and strengthened by CFRP sheets. The predicted-to-measured increase in tendon stress at an ultimate state ratio were drawn for all the equations given in Standards in Figure 6. Overestimates appear as a predicted-to-measured ratio greater than one and the underestimates as less than one.

5. 1. ACI ACI-318-2011 recommends the following equations to determine stress in unbonded tendon at an ultimate state $f_{ps,u}$, that originally proposed by Mattock et al. [20] and later modified by Mojtahedi and Gamble [21] to account for the influence of the span-to-depth ratio:

for $L/d_p \le 35$:

$$\Delta f_{ps,u} = -486.47 + \frac{f_c^{'}}{77.012\rho_p} \le f_{py} \quad \text{MPa} \tag{2}$$

for $L/d_p > 35$:

$$f_{ps,u} = f_{pe} + \Delta f_{ps,u} = f_{pe} + 70 + \frac{f_c^{'}}{300\rho_p} \le f_{py} \tag{3}$$

or $(f_{pe} + 200)$ MPa

where $\Delta f_{ps,u}$ is increase in tendon stress at an ultimate state, f_{pe}effective pre-stress in the pre-stressing steel, $f_c^{'}$compressive strength of concrete, $\rho_p = \dfrac{A_{ps}}{bd_{ps}}$, A_{ps}area of prestressing tendons, $b$width or effective width of the section or flange in the compression zone, d_{ps}depth from concrete extreme fiber to centroid of pre-stressing steel, f_{py}yield strength of pre-stressing steel and Llength of the span.Substituting the average test values of the material strength of the tested beams into Equations (2)-(3) and dividing by the experimental results is shown in Figure 7, the ACI underestimated ultimate tendon stress fps,u, of all tested beams. This is due to the fact that Equations (2)-(3) was derived for fully prestressed simply supported beams and considers only the effect of span-depth ratio, compressive strength of concrete and prestressing reinforcement index, but ignores the effect of strengthened and multi-span or loading pattern in continuous beams.

5. 2. AASHTO LRFD Based on workreported by MacGregor [22] and MacGregor et al. [23] AASHTO LRFD Bridge Design Specification suggests the following equations to determine the stress in unbonded tendon at an ultimate state $f_{ps,u}$:

$$f_{ps,u} = f_{pe} + \Delta f_{ps,u} = f_{pe} + 6300\left(\frac{d_p - c}{\ell_e}\right) \le f_{py}$$
$$\text{MPa} \quad \text{and} \quad \ell_e = \left(\frac{2\ell_i}{2 + N_s}\right) \tag{4}$$

where c is neutral axis depth at ultimate, ℓ_e and ℓ_i are the effective tendon length and length of tendon between anchorages, respectively; and N_s is number of support hinges required to form a mechanism crossed by the tendon. Adopting the average value of the tested strength of the material in the tested beams to Equation (4) and dividing by the experimental results is shown in Figure 6, where all of the data point are under correlation line; thus, Equation (4) predicts conservative values for all tested beams.

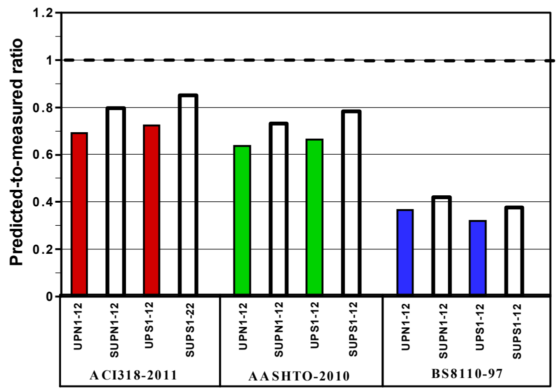

Figure 6. Comparison between experimental and predicted increase in tendon stress of different standards

TABLE 6. Standard error of estimate of different Standards

Standards	ACI (2011)	AASHTO LRFD (2010)	BS (1997)
$S_{y/x}$	197.6	243.1	494.8

5. 3. BS-8110 Considering the investigations carried out by Pannell [24], and Pannell and Tam [25], BS-8110 adopted the Equation (5) to calculate the stress of prestressing in unbonded tendon at the ultimate state:

$$\Delta f_{ps,u} = \frac{7000}{L/d_p}(2.6763 - 90.776\frac{f_{pu}A_p}{f_{cu}bd_p}) \le f_{py} \text{ MPa} \quad (5)$$

where f_{cu} is the strength of concrete taken from cube tests. Similar to the AASHTO, the BS predicts conservative values for all tested beams. However, more conservative results are obtained by BS method.To compare the various equations proposed by mentioned standards, the standard error of estimate $S_{y/x}$, suggested by Chapra et al. [26] is performed. The standard error of estimate produces a single numeric value indicating the spread of all of the population of tests and is expressed by Equation (6):

$$S_{y/x} = [S_r / (n-2)]^{1/2} \quad (6)$$

where:

$$S_r = \sum (f_{ps,uei} - f_{ps,upi})^2 \quad (7)$$

where $f_{ps,uei}$and $f_{ps,upi}$are individual experimental and predicted values of $f_{ps,u}$ and n is the number of data. The results of standard error of estimate is listed in Table 6.The results of standard error of estimate $S_{y/x}$, indicates that, the ACI model provides the smallest standard error of estimate for strengthened and non-strengthened beams; so, ACI model provides better estimates than AASHTO model and AASHTO model provides better estimates than BS for tested beams cast with two types of high strength vibrating and non-vibrating concrete.

6. PRELIMINARY MODIFICATION ON THEORETICAL EQUATIONS TO ACI. AASHTO LRFD AND BS FOR ULTIMATE TENDON STRESS INCREASE OF STRENGTHENED AND NON-STRENGTHENED BEAMS CASTED WITH HSCS

The Theoretical stress increase at an ultimate state $\Delta f_{ps,u}$ in unbonded post-tensioned concrete beams proposed by, ACI. AASHTO LRFD and BS for NSC of non-strengthened beams, used to testify the HSCs strengthened and nonstrengthened continuous beams tested in this report. Figure 7 shows the variation of this theoretical values, $\Delta f_{ps,u}^{th}$ by substituting material strength of tested beams into Eqs. (3-5) and comparing it with the experimentalvalues, $\Delta f_{ps,u}^{exp}$. It is indicated that, all theoretical values are lower than the experimental results in continuous strengthened beams cast with HSSCC and HSNC under a concentrated mid-span load. The reason is: i) the Eqs. (3-5) obtained from the testing data on non-strengthened beams cast with normal strength concrete, and ii) in these Eqs. the effect of all important parameters on ultimate stress in unbonded tendons are not considered.Based on the results of HSCs strengthened and non-strengthened tested beams, the stress increase in the unbonded tendons at ultimate state is predicted as follows:

Case 1: Preliminary modification of ACI (Figure 7 (a))

$$\Delta f_{ps,u} = -486.47 + \frac{f'_c}{77.012\rho_p} \le f_{py} \text{ MPa} \quad (6)$$

Case 2: Preliminary modification of AASHTO LRFD (Figure 7 (b))

$$\Delta f_{ps,u} = 70637(\frac{d_p - c}{\ell_e}) - 3740.1 \le f_{py} \text{ MPa} \quad (7)$$

Case 3: Preliminary modification of BS81-10 (Figure 7 (c))

$$\Delta f_{ps,u} = \frac{7000}{L/d_p}(2.6763 - 90.776\frac{f_{pu}A_p}{f_{cu}bd_p}) \le f_{py} \text{ MPa} \quad (8)$$

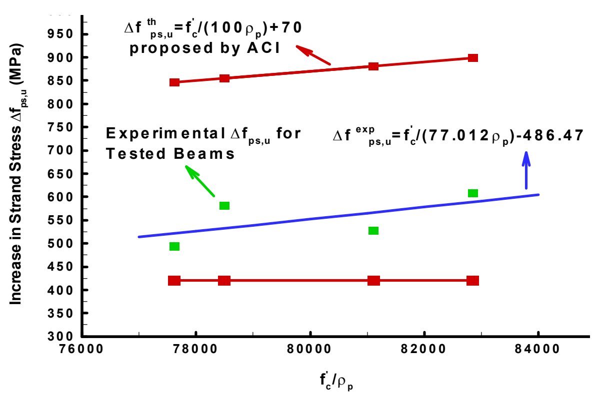

(a)

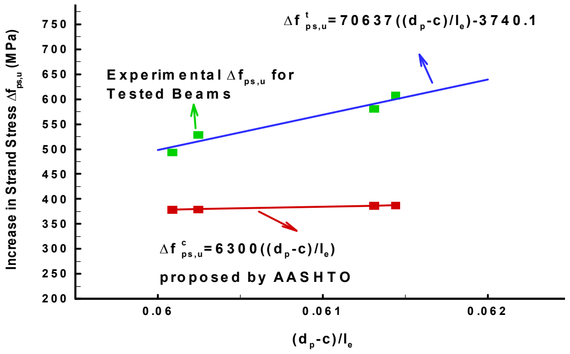

(b)

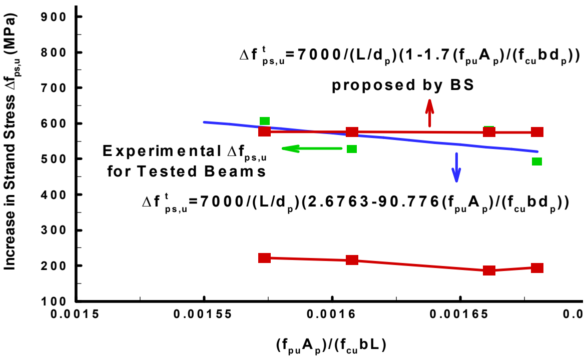

(c)

Figure 7. comparison of experimetal values with theoretical values proposed by different standards

7. CONCLUSION

The increase in tendon's stresses at ultimate ($\Delta f_{ps,u}$) of indeterminate (continuous) strengthened post-tensioned unbonded I-beams consisting of two different type of high strength vibrating HSNC, and non-vibrating concrete, HSSCC were investigated experimentally by testing and monitoring two series of two beams of 9m length.Following results are obtained:

The increase in tendon stress at an ultimate state in strengthened beams consisting of HSC's is lower than non-strengthened beams prepared by HSC's of almost the same concrete strength.

The results of standard error of estimate $S_{y/x}$, indicates that the ACI model provides the smallest standard error of estimate; so, ACI model provides better estimates than AASHTO model and AASHTO model provides better estimates than BS for tested strengthened post-tensioned beams cast with two types of HSCs.

Based on the results of HSCs strengthened and non-strengthened tested beams, the stress increase in the unbonded tendons at ultimate state is given by a preliminary modification to each Standard's equation.

The flexural crack width is significantly reduced with strengthened post-tensioned beams. In the cracked preyield stage and after the yielding of tensile steel, the same crack width was observed for strengthened HSNC and HSSCC beams.

In the uncracked elastic stage, the same behavior was observed for strengthened and non-strengthened beams, indicating very similar beam's stiffness prior to concrete cracking. In the cracked preyield stage, the stiffness and yield load of the CFRP strengthened post-tensioned beams were slightly larger than that of the control beams and significant decreases in beam's stiffness was not observed after yielding the tensile steel at sections of negative and positive moments.

8. ACKNOWLEDGMENTS

The authors are grateful for the financial support of the Prifab Company. Special thanks to Engineer S. Zolghadri, Engineer M. Maghsoudi and Engineer A.R. Dortaj for useful discussions and suggestions.

9. REFERENCES

1. Harajli, M.H., Kanj, M., ''Ultimate flexural strength of concrete members prestressed with unbounded tendons'', ***ACI Structural Journal***, Proceedings, Vol. 88, No.5, (1991), 663-671.
2. Lim, j.H., Moon, J.H., Lee L.H., ''Ultimate stress of unbonded tendon in continuous members'', ***Magazine of Concrete Research***, Vol. 55, No.5, (2003), 461-470.
3. Ozkul, O., Nassif, H., Tanchan, P. and Harajli, M., "Rational approach for predicting stress in beams with unbonded tendons", ***ACI Structural Journal***, Vol. 105, No.3, (2008), 338–347.
4. Yang, K.H., Mun, J.H. , "Flexural capacity and stress in unbonded tendons of post-tensioned lightweight concrete beams", ***Journal of Advances in Structural Engineering***, Vol. 16, No.7, (2013), 1297-1310.
5. He, Z., Liu, Z., "Stresses in external and internal unbonded tendons: unified methodology and design equations", ***ASCE Journal of the Structural Division***, Vol. 136 , (2010), 1055–1065.
6. Zhou, W. and Zheng W., ''Unbonded Tendon Stresses in Continuous Post‑Tensioned Beams''., ***ACI Structural Journal***,Vol., 111, No.3, (2014), 525–536.
7. Maghsoudi, A.A., Arabpour, D.F., ''Application of nanotechnology in self-compacting concrete design'', ***International Journal of Engineering***, Vol. 22, No.3, (2009), 229-244.
8. PCI Self-Consolidating Concrete FAST Team, ''Interim guidelines for the use of self-consolidating concrete in PCI member plants'', PCI Committee Summary Report, ***PCI Journal***, (2003), 14-18.
9. Walraven, J., ''Structural aspects of self-compacting concrete. in 3rd international symposium on self-compacting concrete'', Reykjavik, Iceland, (2003), 15-22.
10. Hashemi, S.H., Rahgozar R., Maghsoudi, A.A., ''Flexural testing of high sttrength reinforced concrete beams strengthened with CFRP sheets'', ***International Journal of Engineering***, Vol. 22, No.2, (2009), 131-146.
11. Dehghani, H., Fadaee, M.j., ''Reliabilty-based torsional design of reinforced concrete beams strengthened with CFRP

laminate", ***International Journal of Engineering,*** Vol. 26, No.10, (2013), 1103-1110.

12. Akbarzadeh, h., Maghsoudi, A.A., ''Experimental and analytical investigation of reinforced high strength concrete continuous beams strengthened with fiber reinforced polymer", ***Journal of Materials and Design,*** Vol. 31, (2010), 1130-1147.
13. ACI 318. ''Building code requirements for structural concrete and commentary", Michigan (USA), *American Concrete Institute*, (2011).
14. Okamura, H. and Ozawa, K., ''Mix-design for self-compacting concrete", ***Concrete Library of JSCE,*** Vol. 25, No.6, (1995), 107-120.
15. Domone, PL., ''Self-compacting concrete: an analysis of 11 years of case studies", ***Cement and Concrete Composites***, Vol. 28, No.2, (2006), 197-208.
16. Askari, D.Y., Maghsoudi, A.A., ''Monitoring and theoretical losses of post-tensioned indeterminate I-beams", ***Magazine of Concrete Research***, Vol. 66, No.22, (2014), 1129-1144.
17. Precast/Prestressed Concrete Institute (PCI), "Interim guidelines for the use of self-consolidating concrete in precast/prestressed concrete institute member plants", TR-6-03. PCI, Chicago, Illinois, (2003).
18. AASHTO, "LRFD bridge design specifications", American Association of State Highway and Transportation Officials, 16. Washington, D.C., (2010).
19. BS 8110, ''Structural use of concrete", Part 1, British Standards Institution, London, UK, (1997).
20. Mattock, A.H., Yamazaki. J., Kattula, B.T., ''Comparative study of prestressed concrete beams, with and without bond", ***ACI Journal***, Proceedings Vol. 68, (1971), 116-125.
21. Mojtahedi, S., Gamble, W.L., ''Ultimate steel stresses in unbonded prestressed concrete", ***Journal of Structural Division, ASCE,*** Vol. 104, (1978), 1159-1165.
22. MacGregor, R.J.G., "Strength and ductility of externally post-tensioned segmental box girders", PhD dissertation, The University of Texas at Austin, (1989).
23. MacGregor, R.J.G., Kreger, M.E., Breen J.E., "Strength and ductility of a three-span externally post-tensioned segmental box girder bridge model", Research report no. 365-3F, Center for Transportation Research, The University of Texas at Austin, Austin, (1989).
24. Pannell, F.N., "Ultimate moment resistance of unbounded prestressed concrete beams", ***Magazine of Concrete Research***, Vol. 21, (1969), 43-54.
25. Tam, A., Pannell, F., "The ultimate moment of resistance of unbounded partially prestressed reinforced concrete beams", ***Magazine of Concrete Research***, V. 28, (1976), 203-208.
26. Chapra, Steven, C. and Canale, Raymond, P., ''Numerical methods for engineers", Second Edition, McGraw-Hill, New York, (1988).

Ultimate Unbonded Tendon Stress in CFRP Strengthened Post-Tensioned Indeterminate I-Beams Cast with HSCs

A. A. Maghsudi, Y. Askari D.

Department of Civil Engineering, Shahid Bahonar University, Kerman, Iran

PAPER INFO

Paper history:
Received 31 August 2014
Received in revised form 14 January 2015
Accepted 30 January 2015

Keywords:
Strengthened
CFRP Sheet
Unbonded Tendons
Stress Increases
High Strength Normal
Self-Compacting Concrete
Continuous Beams

چکیده

بر اساس آزمایش خمشی صورت گرفته برای تیرهای پس‌کشیده سراسری دو دهانه، با کابل بدون پیوستگی و مقاومسازی شده و نشده با الیاف کربن، افزایش تنش در کابل‌ها در مراحل مختلف بارگذاری پایش گردیده است. از آنجاکه بتن خودمتراکم، اختراعی مطلوب در صنعت بتن به شمار می‌آید، لذا آشنائی با تاثیر این نوع بتن بر افزایش تنش در چنین کابل‌هائی امری ضروری است. در مقاله حاضر، آزمایشبارگذاری چهار تیر پیوسته پس کشیده با مقطع I شکل که در دو گروه مجزا ساختهو با نصب انواع کرنش سنج‌های الکتریکیدر حین بارگذاری پایش، و نتایج مربوطهارائهشدهاست. گروه اول، شاملتیرهای (UPN1-12, SUPN1-12) ساخته شده با بتن معمولی مقاومت بالا و گروه دوم شامل تیرهای (UPS1-12, SUPS1-12) ساخته شده با بتن خودمتراکم مقاومت بالا می باشد. همچنین، مقایسه نتایج آزمایشگاهی تیرها با آیین‌نامه‌های مختلف ارزیابی شده و اصلاح مقدماتی در روابط هر یک از آئین نامه‌ها پیشنهاد شده است. نتایج حاصل از تخمین خطای استاندارد ($S_{y/x}$) نشان داد که آیین‌نامهACI318-2011نسبت به آیین‌نامه AASHTO-2010 و آیین‌نامه AASHTO-2010 نسبت به آیین نامه BS 8110-97 تخمین بهتری از تنش در کابل‌های فاقد پیوستگی در حالت نهایی دارد. به علاوه، میزان افزایش تنش در حالت نهایی در تیرهای مقاومسازی شده کمتر از تیرهای مقاومسازی نشده (ساخته شده با بتن مقاومت بالا) می‌باشد

***doi**: 10.5829/idosi.ije.2015.28.03c.03*